Metabolic Signatures of Performance in Elite World Tour Professional Cyclists

Travis Nemkov[1*], Francesca Cendali[1], Davide Stefanoni[1], Janel L. Martinez[2], Kirk C. Hansen[1], Iñigo San-Millán[2,3], Angelo D'Alessandro[1*]

[1]University of Colorado Anschutz Medical Campus, Department of Biochemistry and Molecular Genetics, Aurora, CO, USA

[2]University of Colorado Anschutz Medical Campus, Department of Medicine, Division of Endocrinology, Metabolism and Diabetes. Aurora, CO, USA

[3]University of Colorado, Colorado Springs, Department of Human Physiology and Nutrition, Colorado Springs, CO, USA

Correspondence to:
Travis Nemkov, PhD
Department of Biochemistry and Molecular Genetics
University of Colorado Anschutz Medical Campus
12801 East 17th Ave L18-9122., Aurora, CO 80045
Phone # 303-724-0096

E-mail:travis.nemkov@cuanschutz.edu

Angelo D'Alessandro, PhD
Department of Biochemistry and Molecular Genetics
University of Colorado Anschutz Medical Campus
12801 East 17th Ave L18-9118., Aurora, CO 80045
Phone # 303-724-0096
E-mail: angelo.dalessandro@cuanschutz.edu

Running title: *Metabolomics in Elite Professional Cyclists*

Highlights

- We profiled metabolism of 28 international-level elite World Tour professional male athletes from a Union Cycliste Internationale UCI World Team during training and World Tour multi-stage race;
- Dried blood spot sampling affords metabolomics analyses to monitor exercise performance;
- Determination of lactate thresholds during graded exercise test (GXT) to volitional exhaustion shows a range of from 3.75 to 6.5 watts per kilogram in this group;
- Blood profiles of lactate, carboxylic acids, fatty acids and acylcarnitines differed between different exercise modes (GXT and 180 km aerobic training session);
- Metabolic profiles were affected by stage-specific challenges (sprint vs climbing) during a World Tour multi-stage race, won by one of the athletes monitored.

Summary

To characterize molecular profiles of exertion in elite athletes during cycling, we performed metabolomics analyses on blood isolated from twenty-eight international-level elite World Tour professional male athletes from a Union Cycliste Internationale (UCI) World Team taken before and after a graded exercise test (GXT) to volitional exhaustion and before and after a long aerobic training session. Using dried blood spot collection to circumvent logistical hurdles associated with field sampling, these studies defined metabolite signatures and fold change ranges of anaerobic or aerobic exertion in elite cyclists, respectively. Moreover, established signatures were then used to characterize the metabolic physiology of five of these cyclists that were selected to represent the same UCI World Team during a 7-stage elite World Tour race, one of whom was ultimately the race champion. Collectively, these studies provide a unique view of alterations in the blood metabolome of elite athletes during competition and at the peak of their performance capabilities.

Graphical abstract

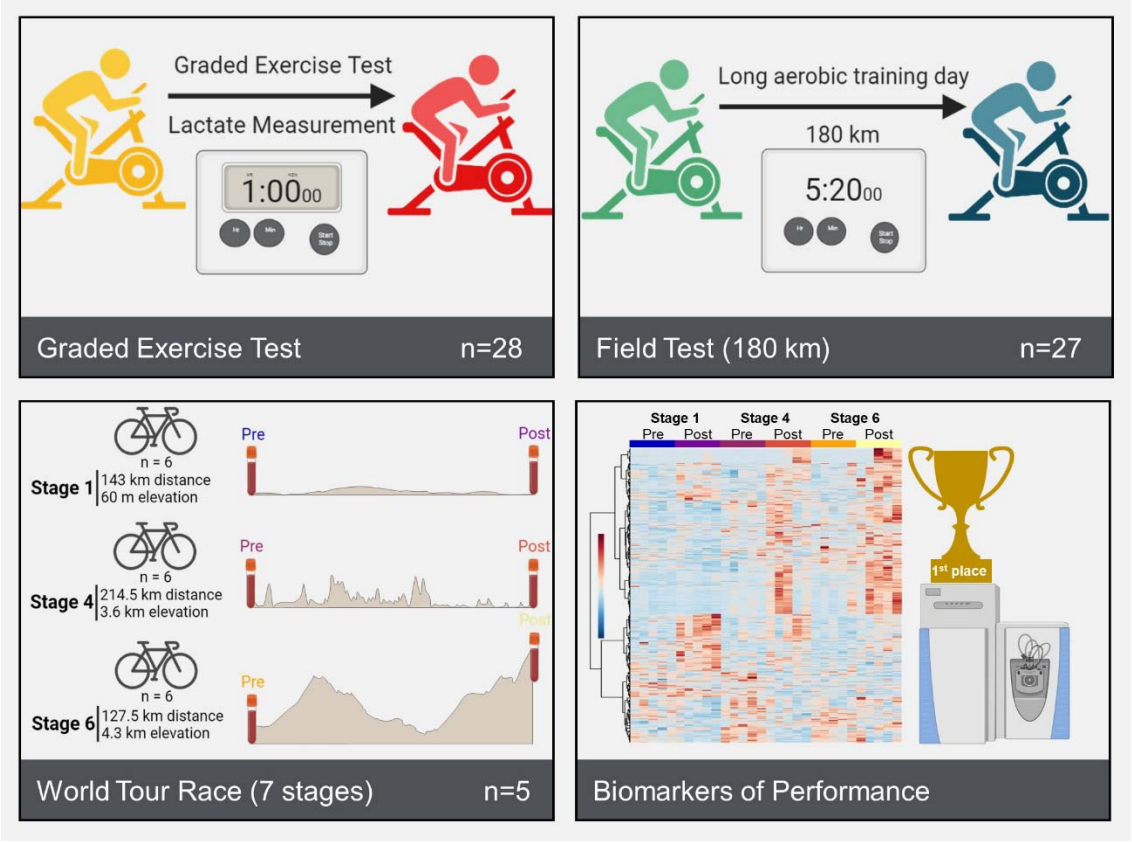

Keywords: **exercise; cycling; bioenergetics; metabolomics; lipidomics; glycolysis; fatty acid oxidation; carnitine**

INTRODUCTION

Investigations into the metabolic effects of exercise (Contrepois et al., 2020; Moghetti et al., 2016) have helped to elucidate physiological adaptations to stress and have been critical for understanding pathologies in which metabolism is dysregulated. From aging (Pontzer et al., 2021) to cardiovascular and other non-communicable diseases (Costantino et al., 2016; Ruiz-Canela et al., 2017), from cancer (Hanahan, 2022) to hemorrhagic or ischemic hypoxia (Chouchani et al., 2014), from immunometabolism (O'Neill et al., 2016) to neurodegenerative diseases (Traxler et al., 2022), metabolic derangements are increasingly appreciated as etiological contributors to disease onset, severity, and prognosis.

Energy requirements and substrate utilization during physical exertion are dependent upon workload and the perfusion of oxygen. During low and medium intensity exercise when oxygen supply is sufficient to meet bioenergetic demands, fatty acid substrates are relied upon for generation of adenosine triphosphate (ATP) through the use of fatty acid oxidation to fuel the Krebs cycle. As exertional intensity increases to a point where oxidative phosphorylation is no longer sufficient, metabolism shifts to favor the rapidity of carbohydrate-driven glycolysis for ATP generation, a metabolic switch that increases the rate of lactate formation. At high glycolytic rates, lactate production exceeds the rate of lactate clearance via mitochondrial metabolism (Brooks, 2018). At this point, lactate is exported into circulation, resulting in increased blood lactate levels. While lactate is mainly formed in fast-twitch fibers, it is oxidized during exercise as a substrate to fuel mitochondria of adjacent slow-twitch muscle fibers. A metabolic inflection point, called the "lactate threshold" (LT), is reached when a maximal effort or intensity that an athlete can maintain for an extended period of time with little or no increase in lactate (Poole et al., 2021). Classic studies have focused on LT as a proxy for exercise performance.

In the last decade, there has been an increased focus on the metabolic responses to exercise including measuring substrate utilization, metabolic flexibility and mitochondrial function in athletes (San-Millán and Brooks, 2018). Recent advances in metabolomics have fostered a more comprehensive understanding of human responses to low, moderate or high intensity exercise (Khoramipour et al., 2022; Sakaguchi et al., 2019). Results have evidenced a differential impact of different exercise modes (e.g., acute versus resistance and endurance exercise (Morville et al., 2020)) and across different sports (e.g., endurance athletes, sprinters, bodybuilders (Al-Khelaifi

et al., 2018; Schranner et al., 2021)) on the extent and magnitude of metabolic reprogramming in recreational athletes. While metabolomics characterization of cycling in recreational (Nemkov et al., 2021) and professional (San-Millán et al., 2020) athletes under controlled acute training regimens has been reported, literature is scarce on elite professional athletes undergoing testing in the field and, more importantly, during World Tour competitions. Performing such investigations in elite professional athletes offers a unique opportunity to determine the ceiling of human performance, against which we can scale human physiology of healthy occasional, recreational, semi-professional and professional athletes. Such scale would also inform a model on how human metabolism works at its optimum, which in turn could drive the interpretation of metabolic derangements under pathological conditions, even at their early onset. Studies on elite athletes also help determining whether and to what extent animal models of exercise (Sato et al., 2022) are translationally relevant.

RESULTS

Metabolomic changes observed in blood vary as a function of training intensity and duration

In consideration that lactate threshold and the shift between substrate and pathway utilization is dependent upon training status, we sought to identify circulating metabolite profiles of aerobic and anaerobic exertion in the whole blood of elite World Tour professional cyclists during a team training camp using mass spectrometry-based metabolomics. To determine lactate threshold, these cyclists were first subjected to a graded exercise test (GXT) to volitional exhaustion, in which progressive increases in power output on an ergometer are accompanied by whole blood lactate measurements (**Figure 1A**). A range of lactate thresholds from 3.75 to 6.5 watts per kilogram was observed in this group, demonstrating variation in metabolic capacity even at the elite level (**Figure 1B**). While heart rate increased as well during the GXT, there only appeared to be small correlations with blood lactate levels and only at lower power outputs (**Supplemental Figure 1**). Guided by the lactate thresholds determined in the GXT, these cyclists subsequently completed a 180 km aerobic training session within a power output range beneath LT (**Figure 1B**). Importantly, guidance on training power output ranges would not be supported by heart rate monitoring alone, as circulating lactate only moderately correlated with heart rate over all measured power output ranges ($R^2 = 0.53$, $p < 0.0001$), and this correlation depended on functional output (**Suppl. Figure 1**). As revealed through metabolomics, blood samples taken before and after the GXT were distinctly grouped by unsupervised Principal Component Analysis (PCA) (**Figure 1D**). Metabolites with the top 15 weights on clustering, as quantified by the variable importance in projection (VIP) score, associated predominantly with glycolysis (pyruvate, lactate), the TCA cycle (malate, succinate), nucleotide and nicotinamide metabolism (xanthine, kynurenic acid, ADP-ribose, phosphate), oxidative stress (cystine, γ-glutamyl-alanine) and fatty acid oxidation (β-hydroxybutyrate, acetylcarnitine, AC (12:0), AC (16:2)) (**Figure 1E**). Meanwhile, PCA of samples taken before and after the long aerobic training session indicated a clear separation between time points with a few samples clustering in the opposite group, possibly indicating varying levels of exertion or recovery (**Figure 1F**). Time points from this training test were predominantly distinguished by acylcarnitines (**Figure 1G**).

In addition to the accumulation of lactate during the GXT (intra-individual fold changes of 2.91±0.94), higher levels of glucose (1.35±0.38), phosphoglycerate (1.48±0.59), phospoenolpyruvate (1.27±0.52), and pyruvate (2.34±0.78), in conjunction with lower levels of

hexose phosphate (0.81±0.50), indicate ongoing glycogenolysis and committal to glycolysis during this exercise (**Figure 1H**). End of test succinate (2.85±1.06) was comparable to lactate accumulation, in addition to higher levels of citrate (1.38±0.61), fumarate (1.36±0.34), and malate (1.66± 0.54) (**Figure 1H**) indicating release into circulation of carboxylic acids. These metabolic profiles were distinct from those observed in the 180 km aerobic training session, given that only glucose (1.17±0.32) and succinate (1.28±0.37) were significantly higher after the test (**Figure 1I**).

Blood profiles of fatty acids and acylcarnitines also differed between these two exercise modes. While long chain fatty acids (LCFA) accumulated during both exercise modes, the extent of accumulation was higher after the 180 km aerobic training session than in the GXT (**Figures 1J** and **1K**). The abundances of short (SCFA) and medium chain fatty acids (MCFA) after the GXT were significantly higher however, suggesting incomplete fatty acid oxidation. In support, post-GXT blood had more abundant short chain acylcarnitines (SCAC), while blood post-180km aerobic training had higher levels of medium chain acylcarnitines (MCAC) and no significant changes to SCAC (**Figure 1L** and **1M**). These findings support more active fatty acid oxidation during the long aerobic training, as further exemplified by lower levels of circulating carnitine 0.86±0.22, in comparison with a ratio of 0.95±0.15 in the MPT (**Figure 1L** and **1M**).

Metabolomic changes vary based on overall progression of multistage World Tour race

We next sought out to determine blood metabolic signatures of selected cyclists from the five members of the UCI elite World Tour Team competing in a World Tour multi-stage race, as a function of both exertion during individual stages and progression throughout the entire competition. Of note, one of the athletes monitored in this study, who cannot be further identified to preserve anonymity, won the overall race. Whole blood samples were collected from 5 competing cyclists prior to and immediately upon completion of Stages 1, 4, and 6, which were characterized by 143 km/60 m, 214.5 km/3,600m, and 127.5 km/4,300m of distance/elevation, respectively, and extracted for metabolomics and lipidomics analysis by high-throughput mass spectrometry (**Figure 2A**). Volcano plots indicated a progressively decreasing number of significant features that were higher at the Pre time point (30, 26, and 11 significant features before the beginning of Stages 1, 4, and 6, respectively) while Stage 6 – the most difficult stage – elicited significant increases in 100 features, followed by 82 significant features after Stage 1,

and 58 significant features after Stage 4 (**Figure 2B**). Untargeted metabolite profiles were hierarchically clustered to assess relative abundances as a function of stage and time (**Figure 2C**). From the untargeted metabolomics data, spectra were manually curated to identify 290 named compounds. Partial-least squares discriminant analysis (PLS-DA) of this sample set separated timepoints chronologically across the Component 1 axis (explaining 16.2% of the variance) (**Figure 2D**, left). Samples obtained from all but one of the cyclists after Stages 4 and 6 begin to deviate from this pattern of progression and spread along the Component 2 axis (describing 6.1% of variance). The top 15 metabolites influencing this pattern according to variable importance in projection (VIP) scores contain primarily amino acids, free fatty acids (FA (20:3, 22:4, 18:1, 16:0, 18:2, 18:3)), and acylcarnitines (AC (16:2)) (**Figure 2D**, right). In light of the progressive separation of Pre and Post time points with respect to Stage, we then analyzed each time point individually. PLS-DA of the Pre time point at Stages 1, 4, and 6 separated each group along Component 1 (12.3% of the variance), with an increased spread of samples taken prior to Stage 6 along the Component 2 axis (12.1% of variance) (**Figure 2E**, left). The top 15 metabolites by VIP score were related to amino acids (glycine, threonine, serine, 3-hydroxyisobutyrate), nitrogen metabolism (N-acetylspermidine), fatty acid metabolism (FA (22:5, 20:3)), glycolysis/energy (glyceraldehyde 3-phosphate, nicotinamide), and oxidative stress/Pentose Phosphate Pathway (PPP) (methionine S-oxide, hexose phosphate, sedoheptulose 7-phosphate) (**Figure 2E**, right). Meanwhile, PLS-DA of the Post time point at Stages 1, 4, and 6 separated each group even more along Component 1 (24.9% of the variance), with two samples taken after Stage 4 that cluster more closely to the post-Stage 6 group of samples (**Figure 2F**, left). The top 15 metabolites by VIP score were enriched in compounds primarily related to fatty acid metabolism, including free fatty acids FA (20:3, 22:4, 6:0, 16:0, 18:0)), in addition to a contribution from amino acids (glycine, asparagine, serine, glutamine), and energy metabolites (GMP, pyruvate, fumarate) (**Figure 2F**, right).

To group molecules based on relative changes throughout the race, we performed c-means clustering (**Figure 2G**). Certain molecules that increased during each stage, though to a lower extent after each subsequent stage are described by cluster 1 (**Figure 2G**, upper left). Pathway analysis of molecules in this cluster identified enrichment in energy (TCA Cycle), anabolism/oxidative stress response (PPP, ascorbate metabolism, methionine and cysteine metabolism), amino acid metabolism (tyrosine, methionine, cysteine, alanine, aspartate), and

protein glycosylation (sialic acid and aminosugar metabolism, N-glycan and keratan sulfate degradation). Metabolites identified in cluster 2 opposed this trend, increasing primarily after the completion of Stages 4 and 6 (**Figure 2G**, upper right). This cluster pertained to oxidative stress (ascorbate metabolism, glutathione metabolism) and energy metabolism (pyridoxine and pyruvate metabolism, glycolysis and gluconeogenesis). Meanwhile, cluster 3 described molecules that are elevated after the completion of Stage 1 and progressively decrease throughout Stage 6 and related primarily to fatty acid activation (**Figure 2G**, lower left). Finally, molecules that decreased after the beginning of the race and did not predominantly recover through Stage 6 were described by cluster 4 and enriched for the metabolism of amino acids, nucleotides, nicotinamide (**Figure 2G**, lower right).

Longitudinal Effects of Cycling on Energy Metabolism

Considering the enrichment of glycolysis, the PPP, and the TCA cycle from the systematic analysis of untargeted metabolomics, we then manually interrogated each of these pathways (**Figure 3A**). Intermediates of the oxidative phase of the PPP including gluconolactone-6-phosphate and 6-phosphogluconate tend to increase after each stage (or significantly increase after Stage 6 or 4, respectively) (**Figure 3B**). Meanwhile, non-oxidative intermediate sedoheptulose 7-phosphate decreased, while the pool of pentose phosphate isobars tended to increase after each stage (**Figure 3B**). At steady state, these results suggest an activation of the PPP in response to cycling, which is supported by a progressive increase in the levels of glucose 6-phosphate during the course of the race (**Figure 3C**). This metabolite serves as a commitment of glucose towards catabolism through the activity of hexokinase to fuel both the PPP and glycolysis. While significant differences in glucose levels were not observed, a trend towards elevated glucose after Stage 1 indicates ongoing glycogenolysis. Utilization of glycolysis is apparent given the trending increase of late-stage glycolytic intermediates upstream of pyruvate and lactate. (**Figure 3C**). Interestingly, the accumulation of lactate after each successive stage is lower, suggesting either a routing of carbon into the mitochondria to fuel oxidative phosphorylation, or a progressive loss in glycolytic capacity in these cyclists as fatigue accumulates. While citrate increases (significantly after Stage 6), the magnitude of significant increases in late TCA cycle intermediates succinate, fumarate, and malate mirror lactate (**Figure 3D**). However, respective amino acid products of transamination reactions (alanine/pyruvate,

aspartate/malate, glutamine/glutamate/α-ketoglutarate) inversely mirror their carboxylate counterparts, suggesting ongoing transamination for anaplerosis and to maintain nitrogen homeostasis (**Figure 3E**).

Longitudinal Effects of Cycling on Lipid Metabolism

In addition to the use of glucose and amino acid-derived carbon to fuel the TCA cycle, fatty acids are often relied upon as a fuel source for energy generation, especially under aerobic conditions of exercise. As such, we performed untargeted and semi-targeted lipidomics to assess the relative levels of lipids during the course of the race (**Figure 3F**). While lipid classes as a whole showed variable patterns and significance, we focused on the longitudinal levels of both free fatty acids and acylcarnitines, which are involved in beta oxidation to generate acetyl-CoA (**Figure 3G**). The levels of free medium chain (C10-14) and long chain (C16-22) fatty acids with varying degrees of unsaturation showed a marked increase after Stages 4 and 6. In similar fashion, the accumulation of MCAC begins to appear after Stage 4 and is more pronounced following Stage 6. The generation of these compounds is dependent in part on the availability of carnitine. This molecule showed a significantly progressive decrease throughout the course of the race, while the levels of the Coenzyme A precursor, pantothenate, remained unchanged aside from a slight, though significant, increase after Stage 4 (**Figure 3H**).

Individual Cyclist Metabolomics as a Function of Performance

The penultimate stage of the race consisted of a 127.5 km course through a mountainous region finishing with a first category climb (7% average grade) over the final 7.5 km (**Figure 4A**). Cyclists 1 and 2 managed to outpace the other 3 throughout this stage, which was driven in part by the final vertical ascent (**Figure 4B**). To identify metabolite signatures that may associate with performance during this period of the race, we correlated metabolite levels from blood sampled immediately after Stage 6 with average speed. Top correlates pertained predominantly to oxidation of fatty acids (AC (18:2), AC (18:1), AC (16:0), AC (18:0), AC (18:3), AC (3:1), FA (6:0), and pantothenate), nitrogen homeostasis (spermine, 5-hydoxyisourate, 5-methylthioadenosine, 4-acetoamidobutanoate, lysine, spermidine), and energy metabolism (glyceraldehyde 3-phopshate, succinate) (**Figure 4C** and **4D**). To expand analysis of personalized metabolic profiles across the entirety of sampling throughout the race, Sparse

Partial Least Squares Discriminant Analysis (sPLS-DA) revealed a similar trend as the speed and output data, with Cyclists 1 and 2 clustering together along the Component 2 axis (explaining 7.8% of the data variance) (**Figure 4E**). The top 10 metabolites that contribute to the clustering pattern along this axis were enriched for intermediates of fatty acid oxidation (**Figure 4F**). Indeed, Cyclists 1 and 2 maintained the highest levels of pantothenate and LCAC, including AC (16:0), AC (18:0), AC (18:1), AC (18:2), and AC (18:3) throughout the duration of Stages 1, 4, and 6 (**Figure 4G**). Cyclist 1 in particular, who ultimately won this Stage and the overall race, demonstrated the highest maintained levels of carnitine, lowest levels of MCAC, and LCFA (**Figure 4G** and **4H**), suggesting maintenance of mitochondrial capacity throughout the race. In support, this cyclist also finished Stage 6 with the lowest levels of glycolytic intermediates, lactate, and succinate (**Figure 4I** and **4J**), along with a larger pool of NAD (H) (**Figure 4K**), indicating a lower fatigue status that could sustain a faster pace towards the end of the race for an overall victory. The same cyclist 1 displayed the highest levels of arginine and polyamines (spermine – **Suppl. Figure 2.A**), argininosuccinate, 5-methylthioadenosine (**Suppl. Figure 1.B**), second highest levels of citrulline, but lowest levels of S-Adenosyl-methionine, creatinine and phosphocreatine (**Suppl. Figure 2.B**) across all other team members throughout the Tour. Most notably, Cyclist 1 showed the highest levels of reduced and oxidized glutathione (total glutathione pools), and methionine as well (**Suppl. Figure 2.C**), suggestive of the highest antioxidant capacity across all cyclists monitored in this study through the competition.

DISCUSSION

Here we used mass spectrometry-based metabolomics and lipidomics to define whole blood molecular profiles associated with sustained low to medium intensity cycling during a 180 km aerobic training ride in comparison with a graded exercise test to volitional exhaustion. To facilitate field sampling, we circumvented the need for maintaining frozen samples as is traditionally required for metabolomics analyses through the implementation of dried blood sampling using volumetric absorptive microsampling (Volani et al., 2017). Because these samples were taken from the same elite professional cyclists during a weeklong training camp prior to the season, they enable a paired comparison of molecular profiles as a function of exertion and define blood profiles of humans performing at optimal capacity. Metabolite profiles of the GXT demonstrated characteristic accumulations of circulating lactate, a biomarker of performance capacity that has been traditionally used to guide training exercise (San-Millán et al., 2009, 2020). In addition, we were able to quantify the extent to which upstream glycolytic intermediates are modulated to sustain lactate production. The accumulation of lactate occurs at a power output when the rate of lactate production exceeds that of oxidation, mostly termed the "lactate threshold," which is dependent upon the ability to oxidize lactate into pyruvate for subsequent metabolism in the mitochondria. (Brooks, 1985, 2018) Exercise intensity dictates demand for ATP and drives skeletal muscle metabolic responses to exercise. At high exercise intensities, glycolysis is the primary source of ATP, which is produced at a faster rate through the activity of glycolytic enzymes phosphoglycerate kinase and pyruvate kinase in comparison to mitochondrial electron transport chain-fueled ATP synthase. The latter route for ATP synthesis is dependent on mitochondrial and fatty acid oxidation capacity, which becomes limiting at higher workloads. Under hypoxic conditions or at high bioenergetic demand, mitochondrial respiration becomes uncoupled leading to an accumulation of succinate, which is released into the extracellular environment (Chouchani et al., 2014; D'ALESSANDRO et al., 2017) as a function of intracellular proton accumulation (Reddy et al., 2020). In line with previous findings (San-Millán et al., 2020), we observed ratio increases in succinate that were comparable to that of lactate during the GXT. During the 180 km training session however, when cyclists are predominantly functioning in aerobic conditions and primarily relying on fatty acid oxidation, succinate shows only modest increases while lactate remained unchanged.

High exercise intensities predominantly promote carbohydrate oxidation, while low and medium intensities rely more upon catabolism of fatty acids for energy generation. Accordingly, we observed a substantially higher accumulation of LCFA including the most abundant oleic and linoleic acid (Buchanan et al., 2021) after the 180 km training session in comparison with the GXT. The relatively higher levels after the long training session indicate a longer period of fatty acid mobilization during this training test, which are subsequently converted intracellularly between acyl-CoA and acylcarnitine species for fatty acid oxidation within the mitochondria. The inability of mitochondria to continue oxidizing fatty acids, either due to lack of oxygen availability or cessation of exercise, results in release of incompletely oxidized MCAC back into circulation. SCAC and MCAC notably accumulated significantly after the GXT in comparison to the lower intensity training session, indicating an abrupt shift in metabolism due to progressively increasing exercise intensity. The resulting accumulation of lactate exerts endocrine and autocrine actions by decreasing lipolysis (Liu et al., 2009) and mitochondrial fatty acid transport through decreased carnitine palmitoyltransferace I and II (CPT I and II) function (San-Millan et al., 2022). Of note, MCAC have higher baseline levels in patients with Type 2 diabetes (Makrecka-Kuka et al., 2017; Sun et al., 2016), sepsis (Langley et al., 2013; Rogers et al., 2014), and post-acute sequelae of SARS-CoV-2 infection (PASC) (de Boer et al., 2022), and indicate that acute exercise-induced fatigue mimics certain aspects of chronic diseases in which metabolic and mitochondrial dysfunction or impairment play an important pathogenic role. .

When translated into a World Tour cycling competition, the metabolomic signatures presented herein enable assessment of workload and performance. For instance, the most significantly enriched pathway in Cluster 1, which described compounds that accumulate the most after Stage 1, was the TCA Cycle. This stage was characterized by long stretches of flat terrain with few hills and finished with a field spring favoring higher workloads, in line with the profiles seen in the GXT to volitional exhaustion. On the other hand, Stages 4 and 6 involved more climbing, and Stage 6 in particular finished at the highest elevation of the race. Moreover, all but 1 of the cyclists we profiled were not in contention to win the race and as such, paced at lower outputs. Accordingly, we observed profiles indicated a predominant reliance on fat oxidation, as reflected by accumulation of fatty acids and medium chain acylcarnitines.

While this study only profiled the longitudinal patterns of 5 professional cyclists, correlation of metabolic profiles with speed revealed interesting patterns. The fastest 2 cyclists finished

Stage 6 with the highest levels of abundant LCAC and the lowest levels of circulating succinate, indicating ongoing aerobic fatty acid oxidation despite generating the highest power output and speed on the final ascent. Longitudinal characterization of all three sampled stages during the race revealed that these cyclists maintained the highest levels of abundant LCAC in this cohort, along with the highest level of CoA precursor pantothenate (Vitamin B5). Furthermore, Cyclist 1, who ultimately won this stage and the race overall, had the lowest level of incompletely oxidized MCAC along with the highest level of carnitine. This cyclist was the lone individual who did not deviate from the sample trajectory determined by PLS-DA (**Figure 2D**), and furthermore maintained the highest lactate threshold measured during training camp (**Figure 1B**). These results indicate that high performing elite cyclists have an increased capacity to maintain mitochondrial metabolism and oxidative phosphorylation at high workloads and substantiate prior findings that cyclists' performance correlates with higher lactate clearance capacity at comparable power output (San-Millán and Brooks, 2018).

Performance has both genetic and environmental influencing factors. Indeed, elite performance does have a basis in intensive training regimens. (Tucker and Collins, 2012) While genetic factors are not as capable of distinguishing elite athletes on their own, combination of GWAS with metabolomics using metabolic quantitative trait loci (mQTLs) analysis has revealed significant features (Al-Khelaifi et al., 2019). One such mQTL is an association between the endocannabinoid linoleoyl ethanolamide and vascular non-inflammatory molecule 1 (VNN1), which functions as a panetheinase that plays an integral role in recycling of pantothenate to promote mitochondrial activity (Giessner et al., 2018). It is therefore interesting to consider the role VNN1, or additional effectors of CoA/carnitine biosynthesis and fatty acid oxidation, may play in the cyclists profiled herein especially in light of the putative association between this pathway and cyclist performance. Ultimately, the complementarity of this approach holds future promise for personalization of training regiments for sports performance and exercise prescription to treat metabolic syndrome (Grundy et al., 2005) and improve cancer survivorship (Hojman et al., 2018; Marker, 2022).

Although limited by its observational nature, these studies provide a unique view into metabolism of elite athletes performing at the best of their abilities. While not anticipated during these studies, one of the athletes we monitored ultimately won this and multiple subsequent World Tour multi-stage events. In addition, multiple cyclists analyzed here, from training camp

to longitudinal sampling during the World Tour competition, have enjoyed multiple subsequent stage wins in the world's top competitions.

MATERIALS and METHODS

Ethical statement: All study procedures were conducted in accordance with the Declaration of Helsinki and in accordance with a predefined protocol that was approved by the Colorado Multiple Institutional Review Board (COMIRB 17-1281). Written informed consent was obtained from all subjects.

Training Camp: Maximal Physiology Test: Twenty-eight international-level elite World Tour professional male cyclists performed a graded exercise test to exhaustion on an electrically controlled resistance leg cycle ergometer (Elite, Suito, Italy). After a 15-minute warm-up, participants started leg cycling at a low intensity of 2.0 $W \cdot kg^{-1}$ of body weight. Exercise intensity was increased 0.5 $W \cdot kg^{-1}$ every 10 minutes as previously described (San-Millán et al., 2009) Power output, heart rate and lactate were measured throughout the entire test and recorded every 10 minutes including at the end of the test.

Blood Lactate concentration measurement: At the end of every intensity stage throughout the graded training period, a sample of capillary blood was collected to analyze both intra- and extra-cellular levels of L-lactate (Lactate Plus, Nova Biomedical, Waltham, MA, USA). Heart rate was monitored during the whole test with a heart monitor (Polar S725x, Polar Electro, Kempele, Finland).

Training Camp: Aerobic Training Session On a separate day of training camp, 27 international-level World Tour professional male cyclists (Tour de France Level) completed a 180 km training ride over 5:20h. During the ride, each cyclist performed 3 climbs at lactate threshold (as determined by the previous maximal physiology test) and then completed the final 40 km at low aerobic intensity.

Blood Sampling for Metabolomics: Twenty µl of whole blood was sampled before and after the Maximal Physiology Test and the aerobic training session using a Mitra® Volumetric Absorptive Sampling (VAMS) device and dried under ambient conditions according to manufacturer's instructions (Neoteryx, Torrance, CA, USA). Samples were individually sealed in air-tight packaging in the presence of a desiccant and shipped under ambient conditions to the

University of Colorado Anschutz Medical Campus. Upon arrival, individual samples were added to 200 µl of methanol:acetonitrile:water (5:3:2 v/v/v) and sonicated for 1 hour. Metabolite and lipid extracts were isolated by centrifugation at 18,000 x g for 10 minutes. Supernatants were separated into autosampler vials.

World Tour Stage Race: Five international-level World Tour professional male cyclists were selected to represent a Union Cycliste Internationale (UCI) World Team and participated to a 7-stage elite World Tour race. Performance parameters such as speed and power output were monitored using Training Peaks (Louisville, CO, USA). Due to logistical constraints, whole blood samples were collected using the TAP device (Seventh Sense Biosystems, Medford, MA) as previously described (Catala et al., 2018) prior to and immediately upon completion of Stages 1, 4, and 6. Samples were frozen in dry ice within 15 minutes of isolation and were maintained under this condition until all samples were collected, upon which they were shipped on dry ice and stored at -80°C until analysis.

Metabolomics - Sample Preparation: Prior to LC-MS analysis, samples were placed on ice and re-suspended with 9 volumes of ice cold methanol:acetonitrile:water (5:3:2, v:v). Suspensions were vortexed continuously for 30 min at 4°C. Insoluble material was removed by centrifugation at 18,000 g for 10 min at 4°C and supernatants were isolated for metabolomics analysis by UHPLC-MS. The extract was then dried down under speed vacuum and re-suspended in an equal volume of 0.1% formic acid for analysis.

Metabolomics - UHPLC-MS data acquisition and processing: Analyses were performed as previously published (Nemkov et al., 2017; Reisz et al., 2019). Briefly, the analytical platform employs a Vanquish UHPLC system (Thermo Fisher Scientific, San Jose, CA, USA) coupled online to a Q Exactive mass spectrometer (Thermo Fisher Scientific, San Jose, CA, USA). The (semi)polar extracts were resolved over a Kinetex C18 column, 2.1 x 150 mm, 1.7 µm particle size (Phenomenex, Torrance, CA, USA) equipped with a guard column (SecurityGuard™ Ultracartridge – UHPLC C18 for 2.1 mm ID Columns – AJO-8782 – Phenomenex, Torrance, CA, USA) using an aqueous phase (A) of water and 0.1% formic acid and a mobile phase (B) of acetonitrile and 0.1% formic acid for positive ion polarity mode, and an aqueous phase (A) of

water:acetonitrile (95:5) with 1 mM ammonium acetate and a mobile phase (B) of acetonitrile:water (95:5) with 1 mM ammonium acetate for negative ion polarity mode. The Q Exactive mass spectrometer (Thermo Fisher Scientific, San Jose, CA, USA) was operated independently in positive or negative ion mode, scanning in Full MS mode (2 μscans) from 60 to 900 m/z at 70,000 resolution, with 4 kV spray voltage, 45 sheath gas, 15 auxiliary gas. Calibration was performed prior to analysis using the Pierce™ Positive and Negative Ion Calibration Solutions (Thermo Fisher Scientific).

Metabolomics – Data analysis: Acquired data was then converted from .raw to .mzXML file format using Mass Matrix (Cleveland, OH, USA). Samples were analyzed in randomized order with a technical mixture injected after every 15 samples to qualify instrument performance. Metabolite assignments, isotopologue distributions, and correction for expected natural abundances of deuterium, ^{13}C, and ^{15}N isotopes were performed using MAVEN (Princeton, NJ, USA). (Melamud et al., 2010) Discovery mode alignment, feature identification, and data filtering was performed using Compound Discoverer 2.0 (Thermo Fisher Scientific). Graphs, heat maps and statistical analyses (either T-Test or ANOVA), metabolic pathway analysis, PLS-DA and hierarchical clustering was performed using the MetaboAnalyst 4.0 package. (Chong et al., 2018) XY graphs were plotted through GraphPad Prism 8 (GraphPad Software Inc., La Jolla, CA, USA). Pathway graphs were prepared on BioRender.com.

Fuzzy c-means clustering was performed using the R package 'Mfuzz' (v2.20.0) using 4 centers, and m value of 1.5, and a min.acore of 0.7.

Metabolite pathway enrichment analysis was performed using the Peaks To Pathways of MetaboAnalyst 5.0. Feature regions identified with tje longitudinal patterns selected from C-Means Clustering were subjected to pathway analysis and enrichments were plotted a pie charts demonstrating pathway enrichment as a function of observed vs total pathway hits.

Acknowledgments Research reported in this publication was funded by the National Institute of General and Medical Sciences (RM1GM131968 to ADA), and R01HL146442 (ADA), R01HL149714 (ADA), R01HL148151 (ADA), R01HL161004 (ADA), and R21HL150032 (ADA) from the National Heart, Lung, and Blood Institute. The content is solely the

responsibility of the authors and does not necessarily represent the official views of the National Institutes of Health.

Authors' contribution ISM, TN, and AD designed the studies. JLM, ISM performed exercise tests and collected the samples in laboratory and field settings. TN, FC, DS, KCH, AD performed metabolomics analyses; TN performed data analyses and prepared figures. TN wrote the first version of the manuscript, which was finalized with AD and reviewed and approved by all co-authors.

Disclosure of Conflict of interest: The authors declare that TN, KCH and AD are co-founders of Omix Technologies, Inc. TN, AD and ISM, are co-founders of Altis Biosciences. AD is a SAB member for Hemanext Inc, Macopharma, and Forma Therapeutics Inc. AD is a consultant for Rubius Therapeutics. All other authors have no conflicts of interests to disclose.

References

Al-Khelaifi, F., Diboun, I., Donati, F., Botrè, F., Alsayrafi, M., Georgakopoulos, C., Suhre, K., Yousri, N.A., and Elrayess, M.A. (2018). A pilot study comparing the metabolic profiles of elite-level athletes from different sporting disciplines. Sports Med. - Open *4*, 2. https://doi.org/10.1186/s40798-017-0114-z.

Al-Khelaifi, F., Diboun, I., Donati, F., Botrè, F., Abraham, D., Hingorani, A., Albagha, O., Georgakopoulos, C., Suhre, K., Yousri, N.A., et al. (2019). Metabolic GWAS of elite athletes reveals novel genetically-influenced metabolites associated with athletic performance. Sci. Rep. *9*, 19889. https://doi.org/10.1038/s41598-019-56496-7.

de Boer, E., Petrache, I., Goldstein, N.M., Olin, J.T., Keith, R.C., Modena, B., Mohning, M.P., Yunt, Z.X., San-Millán, I., and Swigris, J.J. (2022). Decreased Fatty Acid Oxidation and Altered Lactate Production during Exercise in Patients with Post-acute COVID-19 Syndrome. Am. J. Respir. Crit. Care Med. *205*, 126–129. https://doi.org/10.1164/rccm.202108-1903LE.

Brooks, G.A. (1985). Anaerobic threshold: review of the concept and directions for future research. Med. Sci. Sports Exerc. *17*, 22–34. .

Brooks, G.A. (2018). The Science and Translation of Lactate Shuttle Theory. Cell Metab. *27*, 757–785. https://doi.org/10.1016/j.cmet.2018.03.008.

Buchanan, C.D.C., Lust, C.A.C., Burns, J.L., Hillyer, L.M., Martin, S.A., Wittert, G.A., and Ma, D.W.L. (2021). Analysis of major fatty acids from matched plasma and serum samples reveals highly comparable absolute and relative levels. Prostaglandins Leukot. Essent. Fatty Acids *168*, 102268. https://doi.org/10.1016/j.plefa.2021.102268.

Catala, A., Culp-Hill, R., Nemkov, T., and D'Alessandro, A. (2018). Quantitative metabolomics comparison of traditional blood draws and TAP capillary blood collection. Metabolomics Off. J. Metabolomic Soc. *14*, 100. https://doi.org/10.1007/s11306-018-1395-z.

Chong, J., Soufan, O., Li, C., Caraus, I., Li, S., Bourque, G., Wishart, D.S., and Xia, J. (2018). MetaboAnalyst 4.0: towards more transparent and integrative metabolomics analysis. Nucleic Acids Res. *46*, W486–W494. https://doi.org/10.1093/nar/gky310.

Chouchani, E.T., Pell, V.R., Gaude, E., Aksentijević, D., Sundier, S.Y., Robb, E.L., Logan, A., Nadtochiy, S.M., Ord, E.N.J., Smith, A.C., et al. (2014). Ischaemic accumulation of succinate controls reperfusion injury through mitochondrial ROS. Nature *515*, 431–435. https://doi.org/10.1038/nature13909.

Contrepois, K., Wu, S., Moneghetti, K.J., Hornburg, D., Ahadi, S., Tsai, M.-S., Metwally, A.A., Wei, E., Lee-McMullen, B., Quijada, J.V., et al. (2020). Molecular Choreography of Acute Exercise. Cell *181*, 1112-1130.e16. https://doi.org/10.1016/j.cell.2020.04.043.

Costantino, S., Paneni, F., and Cosentino, F. (2016). Ageing, metabolism and cardiovascular disease: Mechanisms of cardiovascular ageing. J. Physiol. *594*, 2061–2073. https://doi.org/10.1113/JP270538.

D'ALESSANDRO, A., MOORE, H.B., MOORE, E.E., REISZ, J.A., Matthew, J., GHASABYAN, A., CHANDLER, J., SILLIMAN, C.C., HANSEN, K.C., and BANERJEE, A. (2017). Plasma succinate is a predictor of mortality in critically injured patients. J. Trauma Acute Care Surg.

Giessner, C., Millet, V., Mostert, K.J., Gensollen, T., Vu Manh, T.-P., Garibal, M., Dieme, B., Attaf-Bouabdallah, N., Chasson, L., Brouilly, N., et al. (2018). Vnn1 pantetheinase limits the Warburg effect and sarcoma growth by rescuing mitochondrial activity. Life Sci. Alliance *1*, e201800073. https://doi.org/10.26508/lsa.201800073.

Grundy, S.M., Cleeman, J.I., Daniels, S.R., Donato, K.A., Eckel, R.H., Franklin, B.A., Gordon, D.J., Krauss, R.M., Savage, P.J., Smith, S.C., et al. (2005). Diagnosis and management of the metabolic syndrome: an American Heart Association/National Heart, Lung, and Blood Institute Scientific Statement. Circulation *112*, 2735–2752. https://doi.org/10.1161/CIRCULATIONAHA.105.169404.

Hanahan, D. (2022). Hallmarks of Cancer: New Dimensions. Cancer Discov. *12*, 31–46. https://doi.org/10.1158/2159-8290.CD-21-1059.

Hojman, P., Gehl, J., Christensen, J.F., and Pedersen, B.K. (2018). Molecular Mechanisms Linking Exercise to Cancer Prevention and Treatment. Cell Metab. *27*, 10–21. https://doi.org/10.1016/j.cmet.2017.09.015.

Khoramipour, K., Sandbakk, Ø., Keshteli, A.H., Gaeini, A.A., Wishart, D.S., and Chamari, K. (2022). Metabolomics in Exercise and Sports: A Systematic Review. Sports Med. Auckl. NZ *52*, 547–583. https://doi.org/10.1007/s40279-021-01582-y.

Langley, R.J., Tsalik, E.L., van Velkinburgh, J.C., Glickman, S.W., Rice, B.J., Wang, C., Chen, B., Carin, L., Suarez, A., Mohney, R.P., et al. (2013). An integrated clinico-metabolomic model improves prediction of death in sepsis. Sci. Transl. Med. *5*, 195ra95. https://doi.org/10.1126/scitranslmed.3005893.

Liu, C., Wu, J., Zhu, J., Kuei, C., Yu, J., Shelton, J., Sutton, S.W., Li, X., Yun, S.J., Mirzadegan, T., et al. (2009). Lactate Inhibits Lipolysis in Fat Cells through Activation of an Orphan G-protein-coupled Receptor, GPR81. J. Biol. Chem. *284*, 2811–2822. https://doi.org/10.1074/jbc.M806409200.

Makrecka-Kuka, M., Sevostjanovs, E., Vilks, K., Volska, K., Antone, U., Kuka, J., Makarova, E., Pugovics, O., Dambrova, M., and Liepinsh, E. (2017). Plasma acylcarnitine concentrations reflect the acylcarnitine profile in cardiac tissues. Sci. Rep. *7*, 17528. https://doi.org/10.1038/s41598-017-17797-x.

Marker, R.J. (2022). Cancer related fatigue mediates the relationships between physical fitness and attendance and quality of life after participation in a clinical exercise program for survivors of cancer. Qual. Life Res.

Melamud, E., Vastag, L., and Rabinowitz, J.D. (2010). Metabolomic Analysis and Visualization Engine for LC−MS Data. Anal. Chem. *82*, 9818–9826. https://doi.org/10.1021/ac1021166.

Moghetti, P., Bacchi, E., Brangani, C., Donà, S., and Negri, C. (2016). Metabolic Effects of Exercise. Front. Horm. Res. *47*, 44–57. https://doi.org/10.1159/000445156.

Morville, T., Sahl, R.E., Moritz, T., Helge, J.W., and Clemmensen, C. (2020). Plasma Metabolome Profiling of Resistance Exercise and Endurance Exercise in Humans. Cell Rep. *33*, 108554. https://doi.org/10.1016/j.celrep.2020.108554.

Nemkov, T., Hansen, K.C., and D'Alessandro, A. (2017). A three-minute method for high-throughput quantitative metabolomics and quantitative tracing experiments of central carbon and nitrogen pathways. Rapid Commun. Mass Spectrom. RCM *31*, 663–673. https://doi.org/10.1002/rcm.7834.

Nemkov, T., Skinner, S.C., Nader, E., Stefanoni, D., Robert, M., Cendali, F., Stauffer, E., Cibiel, A., Boisson, C., Connes, P., et al. (2021). Acute Cycling Exercise Induces Changes in Red Blood Cell Deformability and Membrane Lipid Remodeling. Int. J. Mol. Sci. *22*, E896. https://doi.org/10.3390/ijms22020896.

O'Neill, L.A.J., Kishton, R.J., and Rathmell, J. (2016). A guide to immunometabolism for immunologists. Nat. Rev. Immunol. *16*, 553–565. https://doi.org/10.1038/nri.2016.70.

Pontzer, H., Yamada, Y., Sagayama, H., Ainslie, P.N., Andersen, L.F., Anderson, L.J., Arab, L., Baddou, I., Bedu-Addo, K., Blaak, E.E., et al. (2021). Daily energy expenditure through the human life course. Science *373*, 808–812. https://doi.org/10.1126/science.abe5017.

Poole, D.C., Rossiter, H.B., Brooks, G.A., and Gladden, L.B. (2021). The anaerobic threshold: 50+ years of controversy. J. Physiol. *599*, 737–767. https://doi.org/10.1113/JP279963.

Reddy, A., Bozi, L.H.M., Yaghi, O.K., Mills, E.L., Xiao, H., Nicholson, H.E., Paschini, M., Paulo, J.A., Garrity, R., Laznik-Bogoslavski, D., et al. (2020). pH-Gated Succinate Secretion Regulates Muscle Remodeling in Response to Exercise. Cell *183*, 62-75.e17. https://doi.org/10.1016/j.cell.2020.08.039.

Reisz, J.A., Zheng, C., D'Alessandro, A., and Nemkov, T. (2019). Untargeted and Semi-targeted Lipid Analysis of Biological Samples Using Mass Spectrometry-Based Metabolomics. Methods Mol. Biol. Clifton NJ *1978*, 121–135. https://doi.org/10.1007/978-1-4939-9236-2_8.

Rogers, A.J., McGeachie, M., Baron, R.M., Gazourian, L., Haspel, J.A., Nakahira, K., Fredenburgh, L.E., Hunninghake, G.M., Raby, B.A., Matthay, M.A., et al. (2014). Metabolomic derangements are associated with mortality in critically ill adult patients. PloS One *9*, e87538. https://doi.org/10.1371/journal.pone.0087538.

Ruiz-Canela, M., Hruby, A., Clish, C.B., Liang, L., Martínez-González, M.A., and Hu, F.B. (2017). Comprehensive Metabolomic Profiling and Incident Cardiovascular Disease: A Systematic Review. J. Am. Heart Assoc. *6*, e005705. https://doi.org/10.1161/JAHA.117.005705.

Sakaguchi, C.A., Nieman, D.C., Signini, E.F., Abreu, R.M., and Catai, A.M. (2019). Metabolomics-Based Studies Assessing Exercise-Induced Alterations of the Human Metabolome: A Systematic Review. Metabolites *9*. https://doi.org/10.3390/metabo9080164.

San-Millán, I., and Brooks, G.A. (2018). Assessment of Metabolic Flexibility by Means of Measuring Blood Lactate, Fat, and Carbohydrate Oxidation Responses to Exercise in Professional Endurance Athletes and Less-Fit Individuals. Sports Med. Auckl. NZ *48*, 467–479. https://doi.org/10.1007/s40279-017-0751-x.

San-Millán, I., González-Haro, C., and Sagasti, M. (2009). Physiological Differences Between Road Cyclists of Different Categories. A New Approach.: 733. Med. Sci. Sports Exerc. *41*, 64–65. https://doi.org/10.1249/01.mss.0000353467.61975.ae.

San-Millán, I., Stefanoni, D., Martinez, J.L., Hansen, K.C., D'Alessandro, A., and Nemkov, T. (2020). Metabolomics of Endurance Capacity in World Tour Professional Cyclists. Front. Physiol. *11*, 578. https://doi.org/10.3389/fphys.2020.00578.

San-Millan, I., Sparagna, G.C., Chapman, H.L., Warkins, V.L., Chatfield, K.C., Shuff, S.R., Martinez, J.L., and Brooks, G.A. (2022). Chronic Lactate Exposure Decreases Mitochondrial Function by Inhibition of Fatty Acid Uptake and Cardiolipin Alterations in Neonatal Rat Cardiomyocytes. Front. Nutr. *9*, 809485. https://doi.org/10.3389/fnut.2022.809485.

Sato, S., Dyar, K.A., Treebak, J.T., Jepsen, S.L., Ehrlich, A.M., Ashcroft, S.P., Trost, K., Kunzke, T., Prade, V.M., Small, L., et al. (2022). Atlas of exercise metabolism reveals time-dependent signatures of metabolic homeostasis. Cell Metab. *34*, 329-345.e8. https://doi.org/10.1016/j.cmet.2021.12.016.

Schranner, D., Schönfelder, M., Römisch-Margl, W., Scherr, J., Schlegel, J., Zelger, O., Riermeier, A., Kaps, S., Prehn, C., Adamski, J., et al. (2021). Physiological extremes of the human blood metabolome: A metabolomics analysis of highly glycolytic, oxidative, and anabolic athletes. Physiol. Rep. *9*, e14885. https://doi.org/10.14814/phy2.14885.

Sun, L., Liang, L., Gao, X., Zhang, H., Yao, P., Hu, Y., Ma, Y., Wang, F., Jin, Q., Li, H., et al. (2016). Early Prediction of Developing Type 2 Diabetes by Plasma Acylcarnitines: A Population-Based Study. Diabetes Care *39*, 1563–1570. https://doi.org/10.2337/dc16-0232.

Traxler, L., Herdy, J.R., Stefanoni, D., Eichhorner, S., Pelucchi, S., Szücs, A., Santagostino, A., Kim, Y., Agarwal, R.K., Schlachetzki, J.C.M., et al. (2022). Warburg-like metabolic transformation underlies neuronal degeneration in sporadic Alzheimer's disease. Cell Metab. S1550-4131(22)00313-8. https://doi.org/10.1016/j.cmet.2022.07.014.

Tucker, R., and Collins, M. (2012). What makes champions? A review of the relative contribution of genes and training to sporting success. Br. J. Sports Med. *46*, 555–561. https://doi.org/10.1136/bjsports-2011-090548.

Volani, C., Caprioli, G., Calderisi, G., Sigurdsson, B.B., Rainer, J., Gentilini, I., Hicks, A.A., Pramstaller, P.P., Weiss, G., Smarason, S.V., et al. (2017). Pre-analytic evaluation of volumetric absorptive microsampling and integration in a mass spectrometry-based metabolomics workflow. Anal. Bioanal. Chem. *409*, 6263–6276. https://doi.org/10.1007/s00216-017-0571-8.

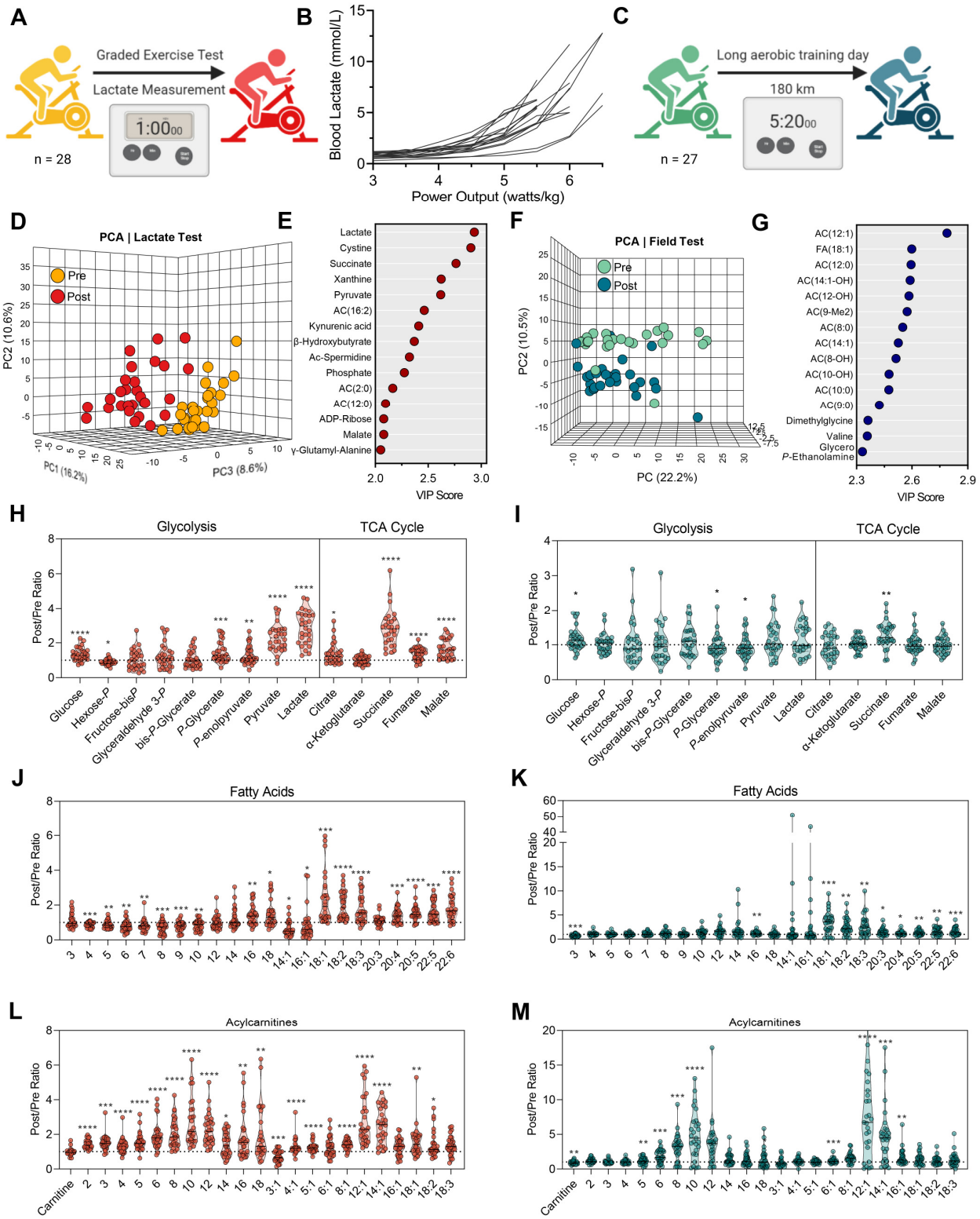

Figure 1 Metabolic signatures of short/high-intensity and long/low-intensity training regimens. (A) During training camp, whole blood from 28 Elite World-Tour cyclists was sampled before and after a one-hour maximal physiology test on an ergometer. (B) Whole blood lactate measurements (mM) as a function of normalized power output (watts/kg) during the test. (C) During the same training camp, whole blood was sampled from 27 of the cyclists before and after a 180 km field test maintained in the Zone 2 regimen. Multivariate analyses including Principal

Component Analysis (PCA) and Variable Importance in Projection (VIP of Partial Least Squares Discriminant Analysis (PLS-DA) were performed on metabolomics data generated from the Max Physiology Test (D) and (E), or Field Test (F) and (G), respectively. Individual cyclist fold changes (Post/Pre) for metabolites involved in glycolysis and the tricarboxylic acid (TCA) cycle are shown as violin plots for the (H) Max Physiology Test and (I) Field Test. Individual cyclist fold changes (Post/Pre) for free fatty acids are shown as violin plots for the (J) Max Physiology Test and (K) Field Test. Individual cyclist fold changes (Post/Pre) for acylcarnitines are shown as violin plots for the (L) Max Physiology Test and (M) Field Test. P-values for Post/Pre comparison are indicated as *<0.05, **<0.01, ***<0.001, ****<0.0001.

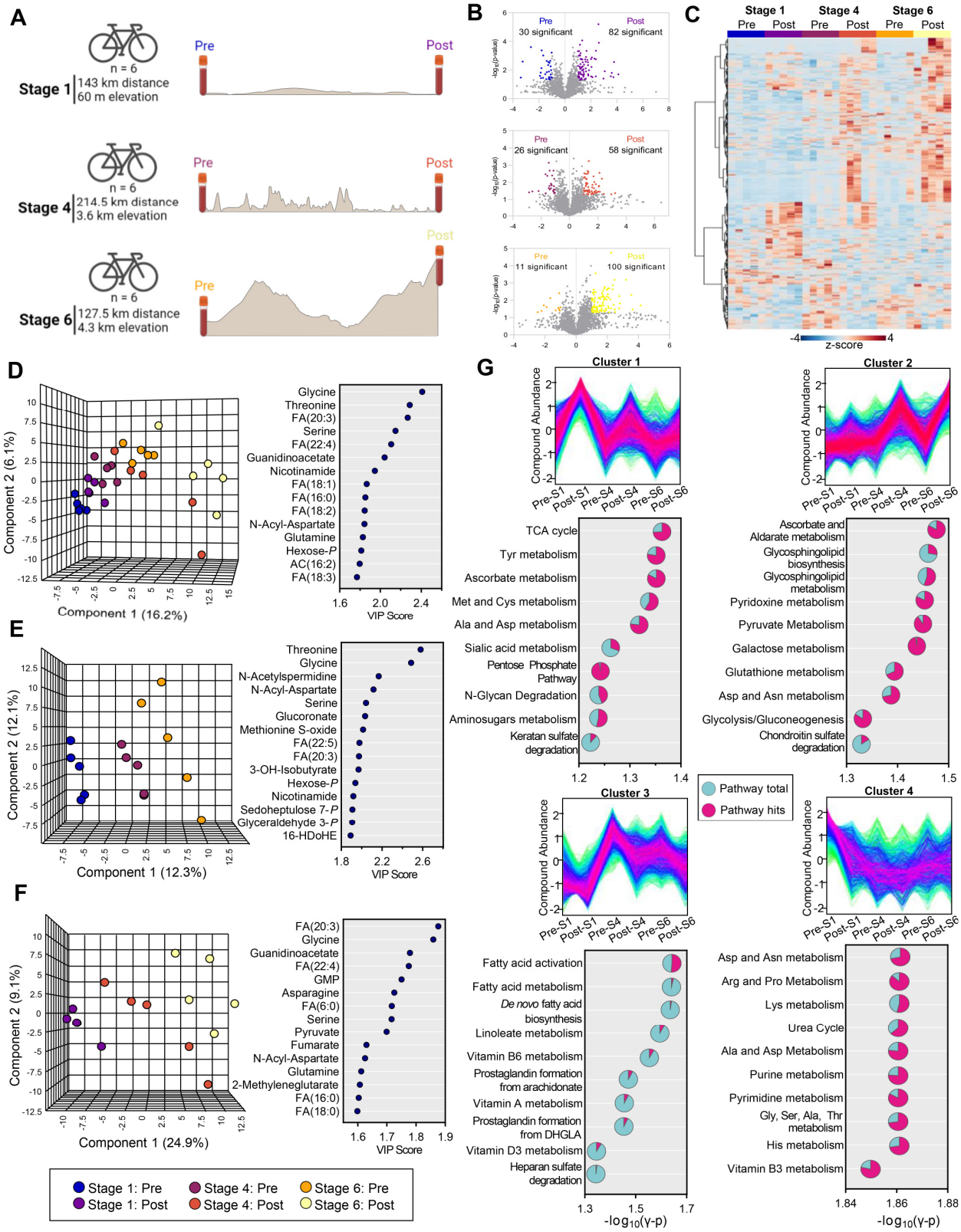

Figure 2 Metabolomics of a multi-stage World Tour cycling race. (A) Whole blood samples were isolated from cyclists before and after Stage 1, 4, and 6 of a consecutive 7 stage race and analyzed by mass spectrometry. (B) Volcano plots for Stage 1, 4, and 6 from top to bottom, respectively, with the number of significantly changed metabolites (fold change>2, $p < 0.05$ indicated in the plot. (C) Hierarchical clustering analysis of each of the features

identified by metabolomics and lipidomics. (D) Partial least squares-discriminant analysis (PLS-DA) of identified metabolites and lipids before and after each stage (left) along with the top 15 compounds by Variable Importance in Projection (VIP) (right). (E) PLS-DA of identified metabolites and lipids before each stage (left) along with the top 15 compounds by VIP (right). (F) PLS-DA of identified metabolites and lipids after each stage (left) along with the top 15 compounds by VIP (right). (G) Four distinct longitudinal signatures were determined by fuzzy c-means clustering. Compounds with patterns matching the top 4 clusters were analyzed to determine significantly enriched pathways in each cluster. Pathways for each cluster are organized by –log10(γ p-value), with number of pathway hits (pink) plotted as a fraction of pathway total (turquoise).

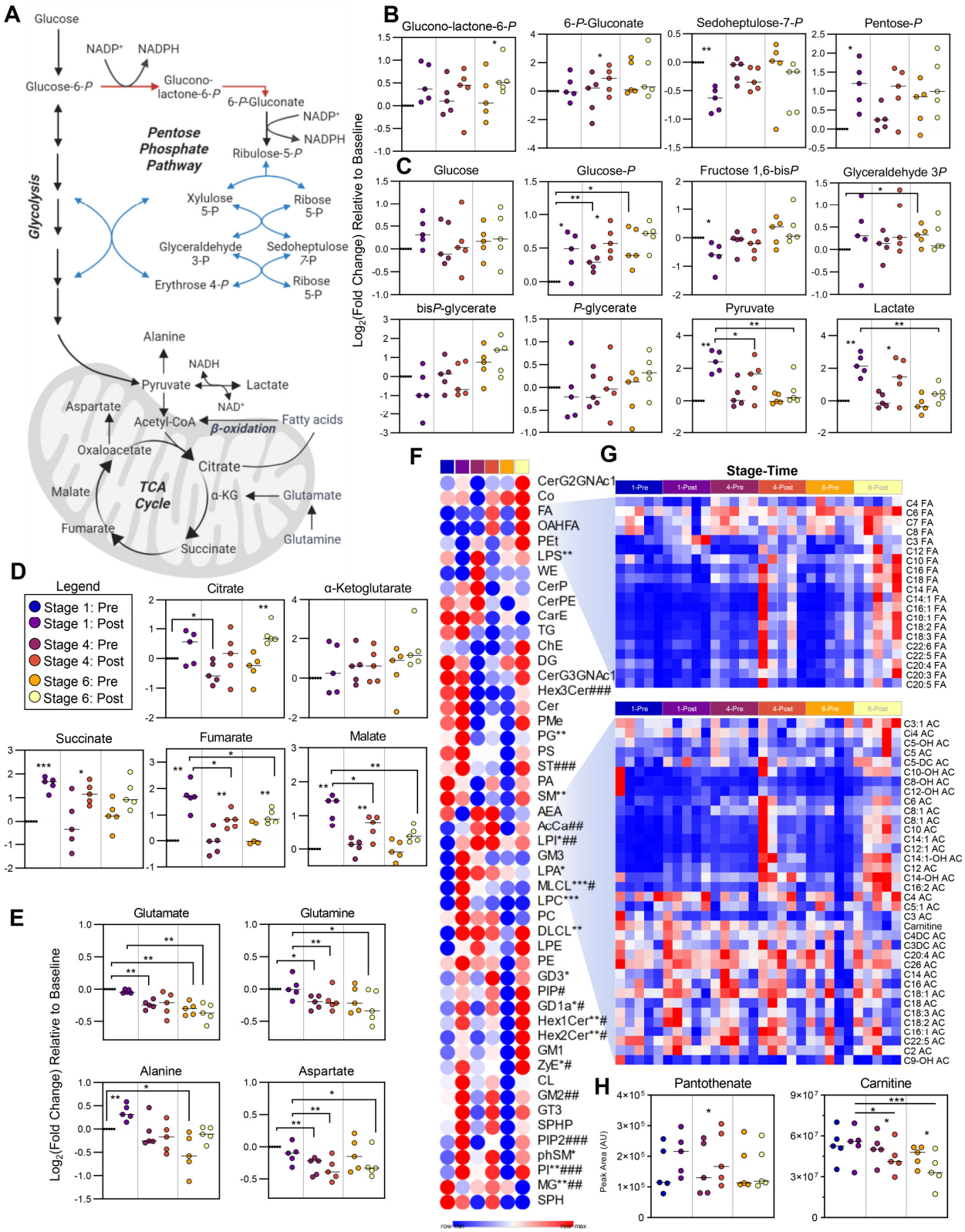

Figure 3 Energy metabolism. (A) A pathway overview of energy metabolism is shown, along with stage comparisons of individual metabolite levels in (B) the Pentose Phosphate Pathway (oxidative phase in red, non-oxidative phase in blue), (C) Glycolysis, and the (D) Tricarboxylic Acid (TCA) Cycle and the (E) amino acid transamination products. p-values are depicted as *<0.05, **<0.01, ***<0.001. (F) A heat map for group averages of the summed total for lipid

classes is shown (lipid abbreviations are provided in the supplemental information). (G Relative levels at each stage/time point of fatty acids (top) and acylcarnitines (bottom) for each cyclist are shown. P-values for Stage 1 Pre/Post comparison (*<0.05, **<0.01, ***<0.001) and Stage 6 Pre/Post comparison (#<0.05, ##<0.01, ###<0.001) are shown. No significant differences for total lipid classes were present in Stage 4 comparisons. (H) The peak areas at each stage/time point for Coenzyme A precursor pantothenate and carnitine are shown.

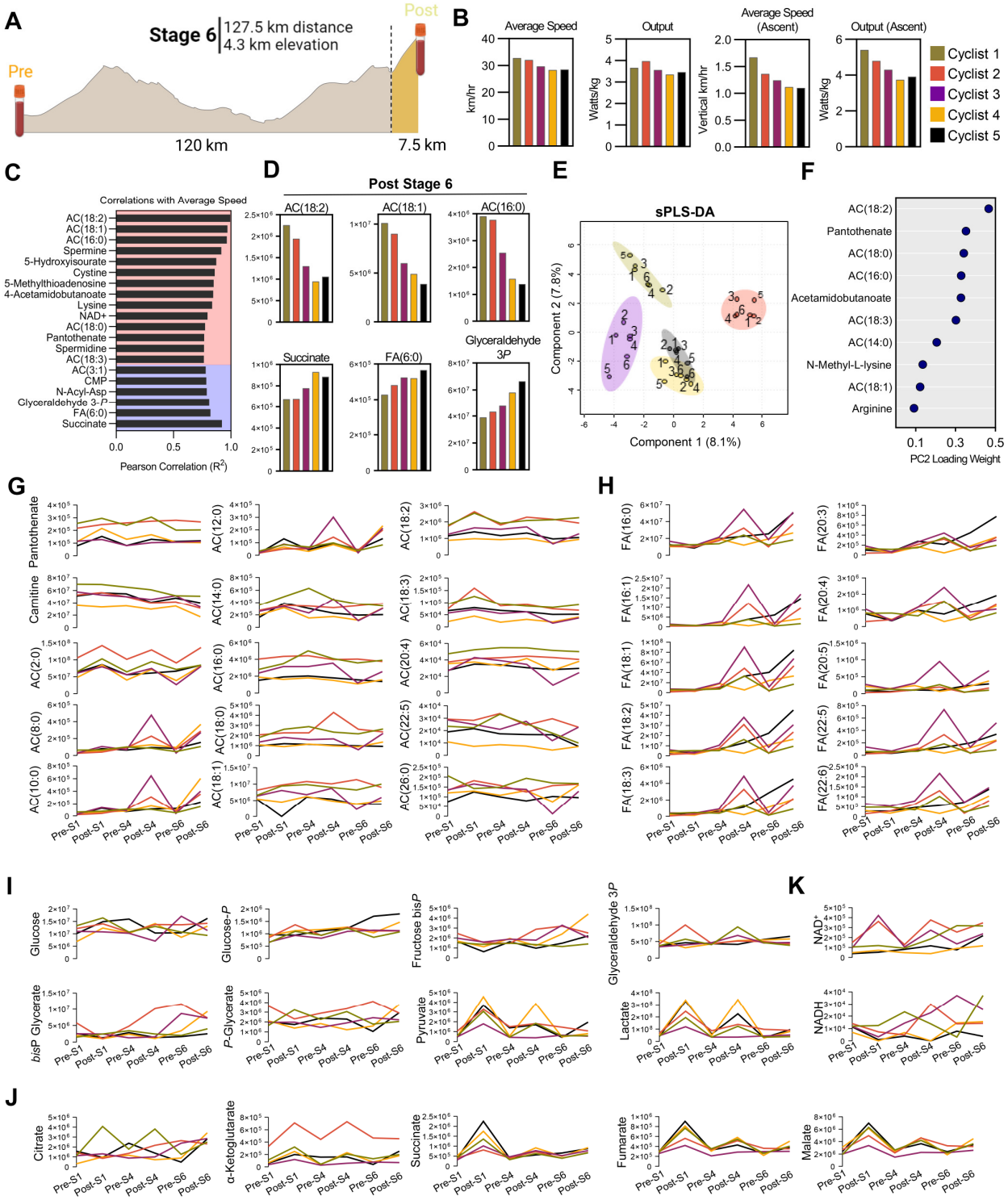

Figure 4 Individual Cyclist Analysis. (A) Metabolite, lipid, and Training Peaks functional cycling data for the entirety of Stage 6, along with Training Peaks during the final 7.5 km climb are analyzed. (B) Average speed and output for Stage 6, as well as the average speed and output of the final 7.5km are plotted by individual cyclist. (C) Sparse Partial Least Squares Discriminant Analysis (sPLS-DA) is shown, with samples color coded according to cyclist and time point indicated as 1-6, where 1 = Stage 1-Pre consecutively up to 6 = Stage 6-Post. (D) The top 10 loadings for principal component 2 are plotted. (E) Pearson Correlation coefficients (R2) for the top 20 Post-Stage 6 metabolite correlates with average speed during Stage 6 are shown, with positive correlates indicated in red

background and negative correlates indicated in blue background. (F) Abundances (y-axis values are peak area top, given in arbitrary units) for each cyclist of the top 3 positive (top) and negative (bottom) correlates with average speed are shown. Longitudinal profiles during the course of the race for (G) acylcarnitines, (H) free fatty acids, (I) glycolysis, (J) TCA cycle, and (K) NAD+/NADH in each cyclist are shown as line graphs, with time points indicated on the bottom x-axis.